Journal of Materials and Environmental Science
ISSN : 2028-2508
e-ISSN : 2737-890X
CODEN : JMESCN

J. Mater. Environ. Sci., 2025, Volume 16, Issue 11, Page 1970-1986

http://www.jmaterenvironsci.com

Evaluating the Feasilibility of Solar powered Irrigation System using Parabolic Dish Concentrator for Rice Cultivation: A Case Study of Abuja, Nigeria

Ajekwe M. Z. [1], Akinsanoye O. A. [3*] and Falode O. A. [1,2],

[1]*Department of Minerals, Petroleum, Energy Economics and Law, Faculty of Multidisciplinary Studies, University of Ibadan, Ibadan; P.M.B 200005, Nigeria.*
[2]*Department of Petroleum Engineering, Faculty of Technology, University of Ibadan, Ibadan; P.M.B 200005, Nigeria.*
[3]*Department of Chemical Sciences, Faculty of Science, Dominican University, Samonda, Ibadan; P.M.B 5361, Nigeria.*

**Corresponding author, Email address: alexolakunle024@gmail.com*

Received *25 Aug 2025,*
Revised *01 Oct 2025,*
Accepted *03 Oct 2025*

Keywords:
- ✓ *Solar Energy;*
- ✓ *Concentrator Solar Power Potential;*
- ✓ *Irrigation;*
- ✓ *Evapotranspiration;*
- ✓ *Parabolic Dish Concentrator*

Citation:*Ajekwe M. Z., Akinsanoye O. A Falode O. A., (2025). Evaluating the Feasibility of Solar Powered Irrigation System using Parabolic Dish Concetrator for Rice Cultivation: A Case Study of Abuja, Nigeria, J. Mater. Environ. Sci., 16(11), 1970-1986.*

Abstract: This study evaluates the feasibility of a solar-powered irrigation system using a parabolic dish collector for rice cultivation in Abuja, Nigeria, to reduce reliance on grid electricity and diesel pumps. This was done by assessing seasonal crop water requirements (SCWR) and Abuja's solar potential to determine system viability.The study was carried out using key meteorological data like solar irradiance, temperature, rainfall and evapotranspiration to estimate the reference crop evapotranspiration (ET_o) by applying this data to the Penman-Monteith equation. At the same time, CWR and Irrigation Water Requirements (IWR) were derived for wet and dry seasons. Solar feasibility is focused on Direct Normal Irradiation (DNI) availability, which is critical for the efficiency of parabolic dish–Stirling engines. The results from the study revealed distinct seasonal variations in evapotranspiration (ET_0) rates which peaks at 4.56 mm/day in February (dry season) and dropping to 2.44 mm/day (wet season). This pattern highlights greater water demand during the dry season, necessitating substantial irrigation, while the wet season's ample rainfall reduced the need for supplemental watering. DNI was strongest in dry months (January, November, and December) but declined during rainy periods due to cloud cover. Abuja's solar potential supports the system though rainy season variability possesses challenges. The study shows that solar – powered irrigation system is a viable alternative to enhance productivity and reduce fossil fuel dependence.

1. Introduction

Nigeria possess abundant renewable energy sources inclusive of solar, wind and hydropower. However, despite the abundance of these resources, energy supply for domestic, industrial and agricultural needs remains a major challenge for the country. The continued reliance on fossil fuels (petrol, diesel etc) and biomass energy (wood) carries substantial economic and environmental costs (Abdalla *et al.*, 2023). The nation's energy sector is faced with two critical challenges; chronic electricity shortages and inadequate sustainable practices with the most severe effects felt in the rural communities. Nigeria's national grid operates at a capacity ranging between $4000MW$ and $7000MW$, with fossil fuels dominating the energy mix at approximately 84%, while renewables is at merely 16%.

This unreliable power supply is a consequence of infrastructural deficiencies and poor grid management, resulting in frequent outages that disproportionately affect rural areas. Consequently, many communities and business are forced to depend on expensive and polluting fossil fuel generators for their electricity needs (Omeje *et al*., 2024). Energy plays a fundamental role throughout the agricultural value chain, yet Nigeria's rural farming sector confronts multiple obstacles. These obstacles include outdated farming techniques, substantial post – harvest losses, inadequate irrigation facilities, heavy reliance on rain – fed agriculture, and the growing impacts of climate change (Alaoui *et al*., 2013; Laita *et al*., 2024). The continued dependence on conventional energy sources like diesel not only increases operational costs but also worsens environmental degradation (Emezirinwune *et al*., 2024),(Omeje *et al*., 2024).

According to Byiringiro *et al.* (2024), solar energy is a clean, sustainable power source that shows great promise for the economy and the environment. Because of its superior energy storage capabilities, concentrated solar power (CSP) technology is more appealing for large-scale power generation. It can meet both thermal and electrical energy demands (Byiringiro *et al*., 2025b). The four technologies that make up CSP are solar power towers, linear Fresnel reflectors, parabolic trough concentrators, and parabolic dish concentrators (Byiringiro *et al*., 2025a). The parabolic dish concentrator can be installed independently, in contrast to other CSP types that need large solar fields and centralized infrastructure. In rural and agricultural areas, where irrigation systems are usually dispersed and situated distant from extensive power networks, this trait is especially beneficial. Furthermore, it provides farmers with a more cost-effective choice for solar-powered irrigation because it is not dependent on intricate and expensive centralized facilities. Due to these numerous benefits, this study aims to evaluate the parabolic dish solar concentrator as a viable option for irrigation in rice farming.

Renewable energy applications in agriculture – including crop drying, livestock water pumping, irrigation systems, food processing, farm lighting, and produce transportation remain underdeveloped despite their enormous potential (Ukoba *et al*., 2024). A wider adoption of renewable technologies in agriculture could reduce farmers' operational costs, minimise greenhouse gas emissions, and promote sustainable agriculture. This transition would support ecological preservation while enhancing economic viability, efficient resource utilisation, and equitable social development (Bathaei and Štreimikienė, 2023; Majeed *et al*., 2023b). This study seeks to address average monthly reference evapotranspiration rates in Abuja using meteorological data such as temperature, solar radiation, and wind speed to optimise irrigation scheduling and water resource allocation for rice cultivation and assess Abuja solar energy potential to determine the feasibility of powering an irrigation system using a parabolic dish solar concentrator coupled with a Stirling engine.

2. Methodology

2.1 Study Area

The study area for this research is Abuja, Nigeria. Abuja ($9.07°N, 7.48°E$) situated in the North-Central region of the country, and at an elevation of $840\,meters$ above sea level. The region experiences two distinct seasons: the wet season and the dry season. The wet season typically occurs between April and October, with rainfall ranging between $1100\,mm$ and $1600\,mm$, while temperatures can reach up to $40°C$. The dry season spans from November to March, characterized by dry winds that can lower temperatures to around $12°C$. The soil characteristics in the study area are primarily influenced by the basement complex and sedimentary rocks, which significantly shape the morphological properties of the local soils (Tanko and Muhsinat, 2014),(Umar *et al*., 2018). Abuja lies within the Guinea Savannah vegetation zone, which, combined with its abundant rainfall and fertile soil, makes agriculture the primary economic activity in the region. Additionally, other economic ventures, such as roofing sheet production and furniture manufacturing, contribute to the local economy. Key crops cultivated in the area include rice, yams, millet, maize, sorghum, cowpea, soybeans, and groundnut (Abubakar, 2014). Strategically, Abuja is located at the geographical centre of Nigeria, at the intersection of two major highways that connect the northern and southern parts of the country. This central positioning makes Abuja more accessible than Lagos, as the distance to all parts of Nigeria is less than $965\,km$. This strategic and central location provides Abuja with a significant economic advantage, fostering connectivity and development (Abubakar, 2014). Figure 1 shows the map of Abuja.

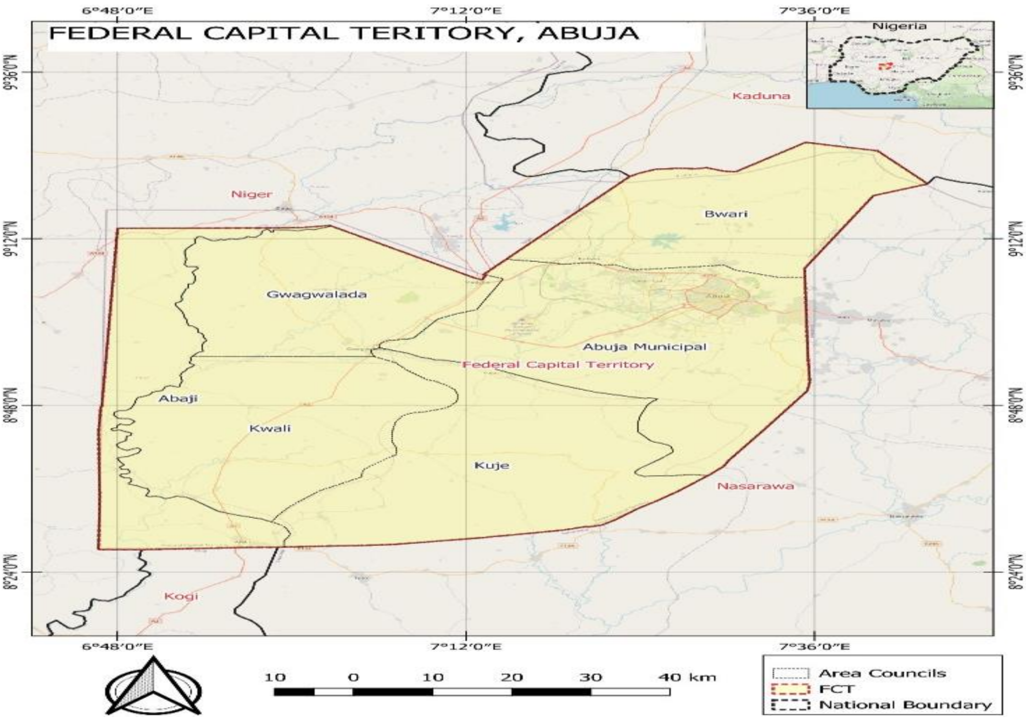

Figure 1. Map of Abuja
Source: Author's Plot using QGIS

2.2 Data Collection

This study utilises data sourced from the National Solar Radiation Database (NSRDB), maintained by the National Renewable Energy Laboratory(NREL) and World weather online, 2024.. The dataset from NSRDB comprises spatial data with of 113,952 rows and 21 columns , where each row corresponds to an hourly interval from 12:30a.m. to 11:30p.m. (24 hrs), recorded at an elevation of 189 meters. The data spans 12 years, from January 1, 2010 to December 31st 2022. For analytical purposes, the dataset was processed to a daily resolution, reducing it to 4740 rows (one per day). Additionally, temperature and wind speed values were adjusted to 2 meter elevation for consistency with standard meteorological references (Allen et al., 1998). The dataset includes key meteorological and solar irradiance data variables such as precitable water, solar zenith angle, surface albedo, Direct Normal Irradiance (DNI), Diffuse Horrizontal Irradiance (DHI), Global Horrizontal Irradiance (GHI), Temperature, Relative Humidity, wind speed e.t.c. World Weather Online is an online API (Application Programming Interface) that has access to historical weather data.

2.3 Estimation of the Reference Evapotranspiration using the Penman – Monteith Equation

The collected data were used to compute the reference crop evapotranspiration (ET_0) by implementing the Penman – Monteith equation in python (Jupyter Notebook). This was done by following the methodology outlined by Zotarelli *et al*., 2013. The Penman – Monteith equation, widely recognized as the standard FAO – 56 model for ET_0 is expressed with Eqn. 1

$$ET_0 = \frac{0.408\Delta(R_n - G) + \gamma\left(\frac{900}{T+273}\right)U_2(e_s - e_a)}{\Delta + \gamma(1 + 0.34U_2)} \qquad \textbf{Eqn. 1}$$

Where ET_0 is the reference evapotranspiration, $[mmd^{-1}]$, R_n is the net radiation at crop surface, $[MJm^{-1}d^{-1}]$, G is the soil heat flux density, $[MJm^{-2}d^{-1}]$, e_s is the saturation vapour pressure, $[kPa]$, e_a is the actual vapour pressure, $[kPa]$, Δ is the slope of the saturation vapour pressure, $[kPa°C^{-1}]$, γ is the psychometric constant, $[kPa°C^{-1}]$, U_2 is the wind speed at 2m height $[ms^{-1}]$, T is the mean daily air temperature, [°C].

Step 1 – Mean daily temperature

The (average) daily maximum and minimum air temperatures in degrees Celsius (°C) were determined using the relation in equation 1.1

Where, T_{mean} = mean daily air temperature, ºC; T_{max} = maximum daily air temperature, ºC; T_{min} = minimum daily air temperature, ºC:

$$T_{mean} = \frac{T_{max} + T_{min}}{2} \qquad \boxed{\text{eqn1.1}}$$

Step 2 – Mean daily solar radiation (R_S)

The average daily net radiation expressed in megajoules per square meter per day (MJ m^{-2} day^{-1}) was determined. A simple average of solar radiation values obtained from a weather station in the period of 24h (0:00:01 am to 11:59:59 pm) was utilised. The conversion of units may be required when solar radiation is expressed in watts per square meter per day (W m^{-2} day^{-1}):

$$Rs_{\,(\mathrm{MJ\ m^{-2} day^{-1}})} = R_{s\,(\mathrm{W\ m^{-2} day^{-1}})} * 0.0864 \qquad Eqn\ 1.2$$

Step 3 – Wind speed (u_2)

The average daily wind speed, measured in meters per second (m/s), at 2m above ground level was determined. It is essential to verify the height at which wind speed is measured, as wind speeds measured at different heights above the soil surface can differ significantly. The wind speed measured at heights other than 2m can be adjusted according to the following equation:

$$u_2 = u_h \frac{4.87}{\ln(67.8\,h - 5.42)} \qquad \boxed{Eqn\ 1.3}$$

Where, $u2$ = wind speed 2 m above the ground surface, m s^{-1};
uz = measured wind speed z m above the ground surface, m s^{-1};
h = height of the measurement above the ground surface, m.
In case the wind speed is given in miles per hour (mi h^{-1}), the conversion to m s^{-1} is required.

$$u_{2\,(m\,s^{-1})} = u2\,(mi\,h^{-1}) * 0.447 \qquad Eqn\ 1.3$$

Step 4 - Slope of saturation vapor pressure curve (î)

For the calculation of evapotranspiration, the slope of the relationship between saturation vapor pressure and temperature, î, is required, hence it was determined using the relation in equation 1.4

$$\Delta = \frac{4098\left[0.6108exp\left(\frac{17.27 * T_{mean}}{T_{mean} + 237.3}\right)\right]}{(T_{mean} + 237.3)^2}$$

$$Eqn\ 1.4$$

T_{mean} = mean daily air temperature, ºC, [Eq.1.4] exp = 2.7183 (base of natural logarithm).

Step 5 – Atmospheric Pressure (P)

The atmospheric pressure, P, is the pressure exerted by the weight of the earth's atmosphere. Evaporation at high altitudes is promoted due to low atmospheric pressure. This effect is, however, small and in the calculation procedures, the average value for a location is sufficient. A simplification of the ideal gas law, assuming 20°C for a standard atmosphere was employed to calculate P in kPa at a particular elevation:

$$P = 101.3\left[\frac{293 - 0.0065z}{293}\right]^{5.26} \qquad Eqn\ 1.5$$

Where,

z = elevation above sea level, m.

P = atmospheric pressure, kPa.

Step 6 – Psychrometric constant (³)

The psychrometric constant relates the partial pressure of water in air to air temperature, allowing vapor pressure to be estimated using paired dry and wet bulb temperature readings. Another way to describe the psychrometric constant is the ratio of specific heat of moist air at constant pressure (Cp) to latent heat of vaporization. The specific heat at constant pressure is the amount of energy required to increase the temperature of a unit mass of air by one degree at constant pressure. Its value depends on the composition of the air, i.e., on its humidity. The average atmospheric conditions of cp value of 1.013 10^{-3} MJ kg^{-1} $°C^{-1}$ was used. As this is done atmospheric pressure is used for each location, the psychrometric constant is kept constant for each location depending of the altitude [Eq.1.6].

$$\gamma = \frac{C_p P}{\varepsilon \lambda} = 0.000665\ P$$

$$Eqn\ 1.7$$

γ = psychrometric constant, kPa °C-1;
P = atmospheric pressure, kPa, [Eq. 10];

λ = latent heat of vaporization, 2.45, MJ kg-1;
c_p = specific heat at constant pressure, 1.013 10^{-3}, MJ kg^{-1} °C^{-1};
ε = ratio molecular weight of water vapour/dry air = 0.622.

Step 7 – Delta Term (DT) (auxiliary calculation for Radiation Term)

In order to simplify the ET_o calculation, several terms are calculated separated. The delta term is used to calculate the "Radiation Term" of the overall ET_o equation (Eq. 1,8):

$$DT = \frac{\Delta}{\Delta + \gamma(1 + 0.34\, u_2)}$$

Eqn 1.8

Where,
Δ = slope of saturation vapor curve; γ = psychrometric constant, kPa °C-1;
u_2 = wind speed 2 m above the ground surface, m s-1.

Step 8—Psi Term (PT) (auxiliary calculation for Wind Term)

The psi term is used to calculate the "Wind Term" of the overall ETo equation [Eq. 1. 9]

$$PT = \frac{\gamma}{\Delta+\gamma(1+0.34u_2)} \qquad Eqn\ 1.9$$

Where,
Δ = slope of saturation vapor curve; γ = psychrometric constant, kPa °C-1;
$u2$ = wind speed 2 m above the ground surface, m s^{-1}.

Step 9—Temperature Term (TT) (auxiliary calculation for Wind Term)

The temperature term is used to calculate the "Wind Term" of the overall ETo equation (Eq 1.10)

$$TT = \left[\frac{900}{T_{mean} + 273}\right] * u_2$$

Eqn 1.10

Where, T_{mean} = mean daily air temperature, ºC.

Step 10—Mean saturation vapor pressure derived from air temperature(e_S)

As saturation vapor pressure is related to air temperature, it can be calculated from the air temperature. The relationship is expressed by:

$$e_{(T)} = 0.6108exp\left[\frac{17.27T}{T + 237.3}\right]$$

Eqn 1.11

Where, $e_{(T)}$ = saturation vapor pressure at the air temperature T, kPa T = air temperature, ºC.

Therefore, the mean saturation vapor pressure is calculated as the mean between the saturation vapor pressure at both the daily maximum and minimum air temperatures Eqn 1.12.

$$e_{(T_{min})} = 0.6108exp\left[\frac{17.27\ T_{min}}{T_{min} + 237.3}\right]$$

$$e_{(T_{max})} = 0.6108exp\left[\frac{17.27\ T_{max}}{T_{max} + 237.3}\right]$$

Eqn 1.13

Where,

T_{max} = maximum daily air temperature, ºC; T_{min} = manimum daily air temperature, ºC;

14

$$e_s = \frac{e_{(T_{max})} + e_{(T_{min})}}{2}$$

The mean saturation vapor pressure for a day, week, decade or month should be computed as the mean between the saturation vapor pressure at the mean daily maximum and minimum air temperatures for that period: Eqn 1.14

Step 11—Actual vapor pressure (ea) derived from relative humidity

The actual vapor pressure can also be calculated from the relative humidity. Depending on the availability of the humidity data, different equations should be used.

$$e_a = \frac{e_{(T_{min})}\left[\frac{RH_{max}}{100}\right] + e_{(T_{max})}\left[\frac{RH_{min}}{100}\right]}{2}$$

Eqn 1.15

Where,

ea = actual vapour pressure, kPa;
$e_{(Tmin)}$ = saturation vapour pressure at daily minimum temperature, kPa;
$e_{(Tmax)}$ = saturation vapour pressure at daily maximum temperature, kPa;
$RHmax$ = maximum relative humidity, %; $RHmin$ = minimum relative humidity, %;

Note I:

a) When using equipment where errors in estimating $RHmin$ can be large, or when RH data integrity are in doubt, use only $RHmax$:

$$e_a = e_{(T_{min})}\left[\frac{RH_{max}}{100}\right]$$

Eqn 1.16

b) In the absence of RH_{max} and RH_{min}:

$$e_a = \frac{RH_{mean}}{100}\left[\frac{e_{(T_{min})} + e_{(T_{max})}}{2}\right] \qquad \boldsymbol{Eqn\ 1.17}$$

Step 12— The inverse relative distance Earth-Sun (dr) and solar declination (δ)

The inverse relative distance Earth-Sun, dr, and the solar declination, δ, are given by:

$$d_r = 1 + 0.033cos\left[\frac{2\pi}{365}J\right]$$
$$\delta = 0.409sin\left[\frac{2\pi}{365}J - 1.39\right]$$

$$\boldsymbol{Eqn\ 1.18}$$

Step 13—Conversion of latitude (φ) in degrees to radians

The latitude, φ, expressed in radians is positive for the northern hemisphere and negative for the southern hemi- sphere (see example below). The conversion from decimal degrees to radians is given by:

$\varphi[Radians] = \frac{\pi}{180}\,\varphi[decimal\ degrees]$ $\quad Eqn\ 1.19$

e.g.1. to convert 13º44N to decimal degrees = 13+44/60 = 13.73

e.g.2. to convert 22º54S to decimal degrees = (-22)+(-54/60)= -22.90

Step 14—Sunset hour angle (ωs)

The sunset hour angle (ωs) is given by:

$$\omega_s = \arccos[-\tan(\varphi)\tan(\delta)] \qquad Eqn1.20$$

Where,

Æ = latitude expressed in radians, [Eq. 25];

¥ = solar declination, [Eq. 24];

Step 15—Extraterrestrial radiation (Ra)

The extraterrestrial radiation, Ra, for each day of the year and for different latitudes can be estimated from the solar constant, the solar declination and the time of the year by:

$$R_a = \frac{24(60)}{\pi} G_{sc} d_r[(\omega_s\ \sin\varphi \sin\delta) + (\cos\varphi\cos\delta\sin\omega_s)]$$

$$Eqn1.21$$

Where,

R_a = extraterrestrial radiation, MJ m^{-2} day-1; G_{SC} = solar constant = 0.0820 MJ m^{-2} min^{-1};

dr = inverse relative distance Earth-Sun; ω_S = sunset hour angle, rad; φ = latitude, rad;

δ = solar declination, rad.

Step 16—Clear sky solar radiation (Rso)

The calculation of the clear-sky radiation is given by equation 1.22:

$$R\text{so} = (0.75 + 2E10^{-5}z) \quad ,Eqn\ 1.22$$

Where:

z = elevation above sea level, m;

Ra = extraterrestrial radiation, MJ m^{-2} day^{-1}

Step 17—Net solar or net shortwave radiation (Rns)

The net shortwave radiation resulting from the balance between incoming and reflected solar radiation is given by:
T_{max} = K maximum absolute temperature during the 24-hour period [K = °C + 273.16],
T_{min} = K minimum absolute temperature during the 24- hour period [K = °C + 273.16],
ea = actual vapor pressure, kPa,
R_S = the incoming solar radiation, MJ m^{-2} day^{-1}; Rso = clear sky solar radiation, MJ m^{-2} day^{-1}.
Where,

$$Rns = (1 - a)Rs \qquad Eqn\ 1.22$$

Rns = net solar or shortwave radiation, MJ m^{-2} day^{-1};

a = albedo or canopy reflection coefficient, which is 0.23 for the hypothetical grass reference crop, dimensionless; Rs = the incoming solar radiation, MJ m^{-2} day^{-1}.

Step 18—Net outgoing long wave solar radiation (Rnl)

The rate of longwave energy emission is proportional to the absolute temperature of the surface raised to the fourth power. This relation is expressed quantitatively by the Stefan-Boltzmann law. The net energy flux leaving the earth's surface is, however, less than that emitted and given by the Stefan-Boltzmann law due to the absorption and downward radiation from the sky. Water vapor, clouds, carbon dioxide and dust are absorbers and emitters of longwave radiation. It is thereby assumed that the concen trations of the other absorbers are constant:

$$R_{nl} = \sigma\left[\frac{(T_{max}+273.16)^4+(T_{min}+273.16)^4}{2}\right]\left(0.34-0.14\sqrt{e_a}\right)\left[1.35\frac{R_s}{R_{so}}-0.35\right]$$

$$Eqn\ 1.23$$

Where,

Rnl = net outgoing longwave radiation, MJ m^{-2} day^{-1},

σ = Stefan-Boltzmann constant [4.903 10^{-9} MJ K^{-4} m^{-2} day^{-1}],

T_{max} = K maximum absolute temperature during the 24-hour period [K = °C + 273.16],

T_{min} = K minimum absolute temperature during the 24- hour period [K = °C + 273.16],
ea = actual vapor pressure, kPa,

R_S = the incoming solar radiation, MJ m^{-2} day^{-1};
Rso = clear sky solar radiation, MJ m^{-2} day^{-1};

Step 19—Net radiation (R_n)

The net radiation (R_n) is the difference between the incoming net shortwave radiation (R_{ns}) and the outgoing net longwave radiation (R_{nl}):

$$R_n = R_{ns} - R_{nl} \qquad Eqn\ 1.24$$

Where,

R_{ns} = net solar or shortwave radiation, MJ m^{-2} day^{-1};
R_{nl} = net outgoing longwave radiation, MJ m^{-2} day^{-1}.
To express the net radiation (Rn) in equivalent of evaporation (mm) (Rng);

$$Rng = 0.408 \times Rn \qquad Eqn\ 1.25$$

Where,
Rn = net radiation, MJ m^{-2} day^{-1};

Final Step—Overall ET_O equation FS1. Radiation term (ET_{rad})

$$ET_{rad} = DT \times Rng \qquad Eqn\ 1.26$$

Where,
ETrad radiation term, mm d-1; DT Delta term; Rng net radiation, mm.

FS2. Wind term (ETwind) $\boldsymbol{Eqn\ 1.27}$

$$ET_{wind} = PT \times TT\,(e_s - e_a)$$

Where,
ET_{wind} = wind term, mm d-1; PT = Psi term; TT = Temperature term;
e_a = actual vapor pressure, kPa;
e_s = mean saturation vapor pressure derived from air temperature, kPa.

Final Reference Evapotranspiration Value (ET_O)

$$Eqn\ 1.28 \qquad ET_o = ET_{wind} + ET_{rad}$$

Where,
ET_o = reference evapotranspiration, mm d-1; ET_{wind} = wind term, mm d-1;
ET_{rad} = radiation term, mm d-1;

Useful Conversions
1 mm = 0.03937 in
1 mm d^{-1} = 2.45 MJ m^{-2} day^{-1}
1 J cm-2 d-1 = 0.01MJ m^{-2} day^{-1}
1 calorie = 4.1868 J
1 cal cm^{-2} d-1 = 4.1868 * 10-2 MJm^{-2} day^{-1}
1 W = 1 J s-1
1W m^{-2} = 0.0864 MJ m^{-2}
°C = (°F –32) 5/9
Kelvin (°K) = (°C) + 273.16
1 millibar (mbar) = 0.1 kPa
1 bar = 100 k Pa
1 cm of water = 0.09807 kPa
1 mm of mercury (mmHg) = 0.1333 kPa 1 atmosphere (atm) = 101.325 kPa
1 lb/in-2 (psi) = 6.896 kPa
1 kilometer day-1 (km d^{-1}) = 0.01157 m s-1 1 ft s^{-1} = 0.3048 m s-1

2.4 Estimation of Crop Water Requirements (CWR) and Irrigation Water Requirements (IWR)

CWR is the water needed to compensate for evapotranspiration(ET) and sustain optimal crop growth. This value is dependent on climatic conditions [temperature, wind , humidity], crop characteristics [growth stage, type], and Phenological stage [initial, development, mid – season and late stages](Allen *et al*., 1998).The CWR can be computed using the **Eqn. 2**

$$CWR = ET_{c,i} = \sum_{i=1}^{m} K_{c,i} \times ET_{o,i} \qquad \textbf{Eqn. 2}$$

Where $ET_{c,i}$ is the daily crop requirement,[mm],$ET_{0,i}$ is the reference evapotranspiration,[mmd^{-1}] $K_{c,i}$ is the crop coefficient for the i[th] day. The process for getting the daily $K_{c,i}$ is described in (Allen *et al*., 1998), i and m represent the first and last days of irrigation in each month.

Rice cultivation in Abuja's tropical savannah climate has distinct wet (April – October) and dry (November – March) seasons. In order to compute the IWR, **Eqn. 3** (Dastane, 1978) will be implemented to get the effective rainfall which will now be used to compute the monthly IWR value using **Eqn. 4** (Brouwer and Hiebloem, 1986).

$$P_e = 0.8 \times \mathrm{P} \qquad \textbf{Eqn. 3}$$

Where P_e is effective rainfall, and P is rainfall.

$$IWR_{monthly} = CWR - P_e \qquad \textbf{Eqn. 4}$$

Where $IWR_{monthly}$ is the monthly Irrigation Water Requirement for rice,[mm] CWR is the Crop Water Requirement for Rice,[mm] and P_e is the effective rainfall [mm].

Considering that some of the water used for irrigation may be lost due to percolation or run – off, hence to minimise the losses, the gross IWR will be calculated using Eqn. 5 (Martin *et al*., 1993).

$$IWR_{gross} = \frac{IWR_{monthly}}{\eta_{eff}} \qquad \textbf{Eqn. 5}$$

Where IWR_{gross} is the gross Irrigation Water Requirement for rice, $IWR_{monthly}$ is the monthly Irrigation Water Requirement for rice,[mm], η_{eff} is the efficiency of surface irrigation in %.

The total IWR for dry season is calculated as the cumulative sum of the monthly gross IWR values as expressed in **Eqn. 6**

$$IWR_{Total} = \sum_{i=1}^{n} IWR_{gross} \qquad \textbf{Eqn. 6}$$

Where IWR_{Total} is the total Irrigation Water Requirement during the entire dry season[mm], IWR_{gross} is the monthly gross Irrigation Water Requirement for dry season months,[$mm/month$], n is the total number of months in the dry season.

2.5 Solar Energy Potential

To comprehensively evaluate the solar energy potential of Abuja in Nigeria, this study analyze solar irradiance data across multiple temporal scales which include hourly variations to identify diurnal patterns, monthly trends to assess seasonal fluctuations and annual averages to determine long-term solar resource availability. This multi-temporal analysis incorporates both Global Horizontal Irradiation (GHI) and Direct Normal Irradiation (DNI) measurements to account for diffuse and direct solar radiation components.nj;

3. Results and Discussion

3.1 Average Monthly Evapotranspiration (ET_0), Irrigation Water Requirement (IWR) and implications for Water Resource Management

The study computed the average monthly evapotranspiration (ET_0) in Abuja using the Penman-Monteith equation, revealing distinct seasonal patterns. **Table 1** confirmed February has the highest ET_0 value ($4.56\ mm/day$) and August the lowest ($2.44\ mm/day$). This implies that high solar radiation and temperatures occur during the dry season (November–March), while the wet season (April–October) experiences substantial rainfall which reduces the need for additional irrigation resulting in lower evapotranspiration rates. This suggests that the dry season produces high solar radiation than the wet season. These observations underscore the need for adaptive irrigation strategies to address seasonal water demands.Irrigation Water Requirements (IWR) followed similar trends, with the dry season (particularly January–March and November–December) showing minimal rainfall and higher irrigation needs. In contrast, the wet season (May–October) provided sufficient water for rice cultivation, with August recording the lowest IWR due to peak precipitation (366.80 mm) as shown in **Table 2a and Table 2b**.

Table 1. Average Monthly Evapotranspiration

Month	Evapotranspiration (ET_0)
January	4.07
February	4.56
March	4.30
April	3.79
May	3.26
June	2.84
July	2.49
August	2.44
September	2.56
October	2.97
November	4.05
December	3.95

Source: Authors Calculations

Table 2a. Monthly Average Rainfall and Average Rainfall Days

Month	Avg. Rainfall (mm)	Avg. Rainfall Days
January	0.40	0.00
February	4.10	1.00
March	13.50	1.00
April	50.50	5.00
May	123.70	9.00
June	154.10	12.00
July	248.20	18.00
August	366.80	21.00
September	320.30	21.00
October	111.40	14.00
November	8.00	1.00
December	0.00	0.00

Source: (World Weather Online, 2024)

Table 3b. Irrigation Water Requirements

Month	IWR (mm/day)
January	226.80
February	247.51
March	221.54
April	204.43
May	102.69
June	96.28
July	89.64
August	87.84
September	89.86
October	80.99
November	0.00
December	123.48

Source: Author's Calculations

These findings offer significant implications for water resource management, demonstrating how evapotranspiration (ET_0) data can enhance precision irrigation by enabling crop-specific scheduling that minimizes both water waste and drought stress. These seasonal water demand patterns provide policymakers with critical insights for equitable resource allocation across agricultural, industrial, and domestic sectors, particularly during the water-scarce dry season. Furthermore, the data reveal climate variability's direct impact on water availability, supporting the development of climate-resilient agricultural strategies. Importantly, the integration of ET_0 and rainfall data with renewable energy systems allows for proper solar-powered irrigation designs that synchronise energy production with cyclical water demands, creating a sustainable approach to water–energy–food nexus challenges in variable climates.

3.2 Solar Irradiation Patterns and Irrigation Implications

Analysis of solar irradiance data reveals distinct temporal patterns: hourly distributions in **Figure 2** show peak GHI and DNI occurring between 12:30p.m. – 1:30p.m., with DHI peaking slightly later (1:30p.m.– 2:30p.m.), while DNI demonstrates greater morning/evening variability due to solar zenith angle effects.

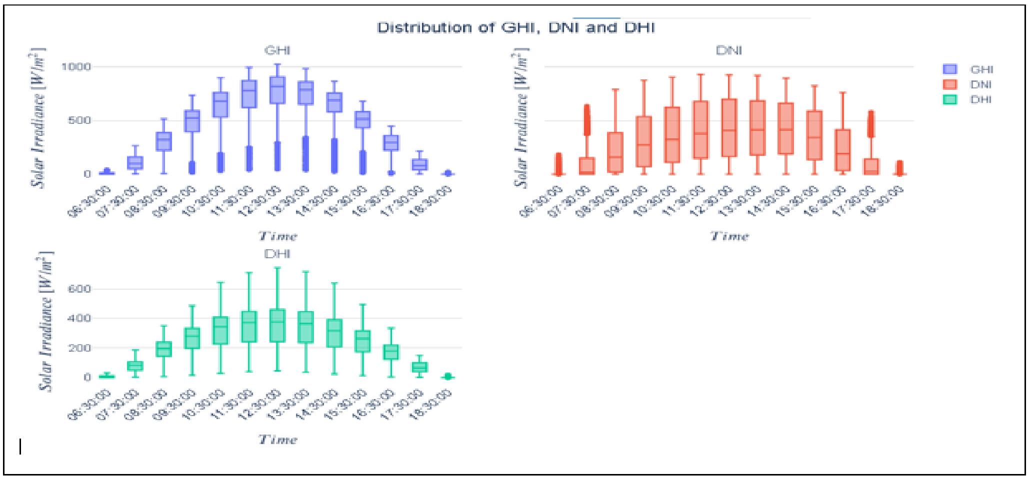

Figure 2. Distribution of Hourly Irradiance
Source: Author's Plot using Python (Jupyter Notebook)

Figure 3 show that monthly trends indicate optimal DNI conditions for Stirling engine operation during January, November, and December, with reduced output between July-August coinciding with rainy season irrigation needs. Annual data confirms stable irradiation patterns, with GHI (~2000 kWh/m²), DNI (~1300 kWh/m²), and DHI (~1000 kWh/m²) maintaining consistent averages over 12 years as shown in **Figure 4**. **Figure 5** shows seasonal sunshine duration varies significantly, averaging 9 hours in dry months (peaking at 10 hours in December) versus 6 hours during wet seasons.

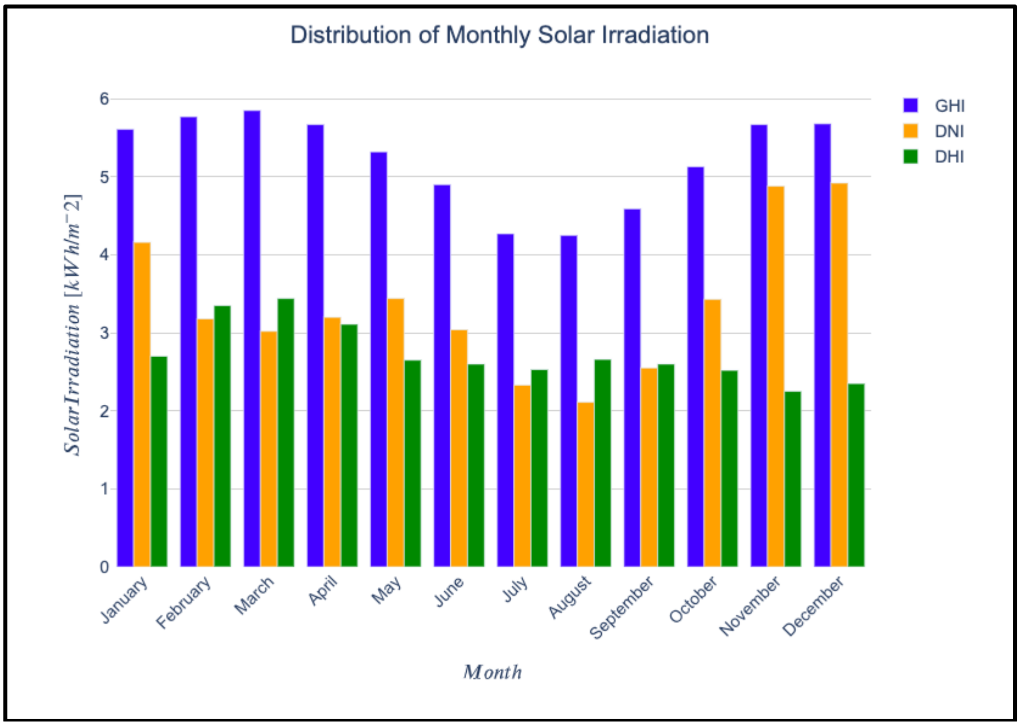

Figure 3. Distribution of Monthly Solar Irradiation
Source: Authors Plot using Python (Jupyter Notebook)

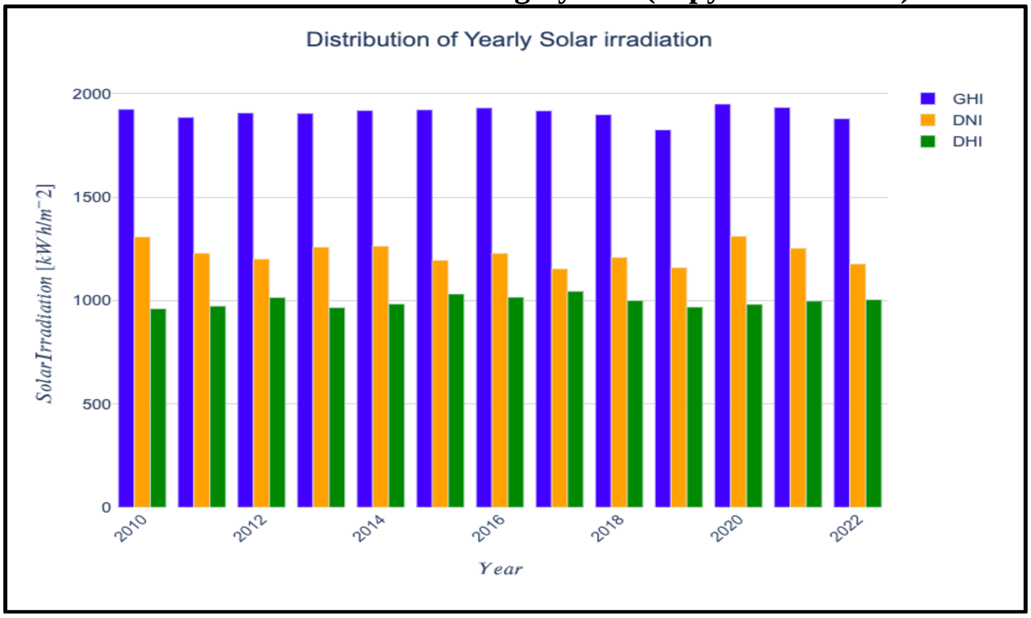

Figure 4. Distribution of Yearly Solar Irradiation
Source: Author's Plot using Python (Jupyter Notebook)

These patterns identify 10:30a.m. – 3:30p.m. as the optimal irrigation window when DNI availability aligns with crop water demands, while the system's natural complementarity - low solar yields during high–rainfall periods - ensures year-round water availability without requiring energy-intensive solutions. The demonstrated irradiance stability supports the long-term viability of the system for agricultural applications.

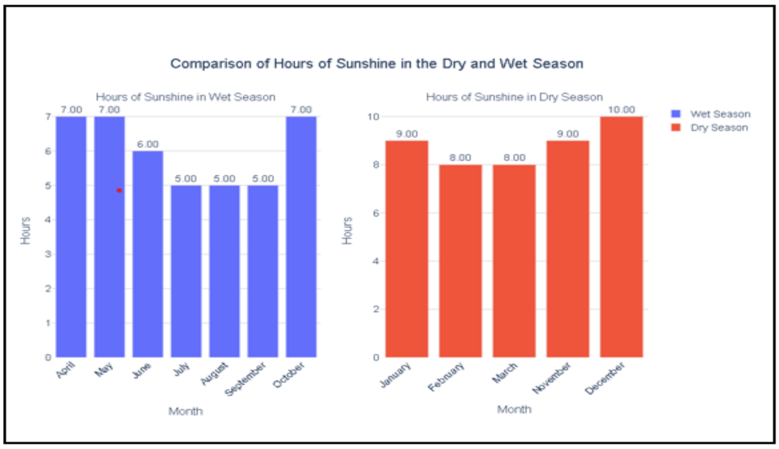

Figure 5. Average Sunshine Hours
Source: Author's Plot using Python (Jupyter Notebook)

4. Conclusion and Recommendation

The study demonstrates the viability of a solar – powered irrigation system using parabolic dish collector for rice cultivation in Abuja, Nigeria. The analysis of evapotranspiration (ET_0) and solar irradiation data reveals a natural synergy between seasonal water demands and solar energy availability. During the dry season (November – March) , when evapotranspiration peaks (at $4.50\ mmd^{-1}$), irrigation needs peak at $247.51\ mm$ as well. Abuja's high Direct Normal Irradiation (at average of about $4\ kWh/m^2$ in the dry season), ensures sufficient energy for pumping, while wet–season rainfall (April – October) reduces reliance on supplemental irrigation. The system's alignment with climatic patterns can be a sustainable solution to Nigeria's energy and food security challenges , eliminating diesel dependence and enhancing agricultural resilience especially when done in large scale

During the wet season, Direct Normal Irradiance (DNI) values drop significantly, limiting the system's efficiency. However, rainfall during this period supplies 80–90% of the irrigation water needed, reducing reliance on solar-powered pumping. For applications beyond irrigation—such as electricity generation and sale—the system should incorporate thermal energy storage (TES) or hybrid renewable systems (e.g., CSP–biogas or CSP–PV) to mitigate intermittency during cloudy or rainy periods.

To facilitate adoption, policymakers should implement targeted subsidies, farmer training programs, and localised pilot projects, particularly in regions with similar savanna climates. Further research should focus on adaptive system designs for diverse crops and geographies, utilising advanced forecasting tools like machine learning to optimise performance. This scalable approach can strengthen the water–energy–food nexus across Sub-Saharan Africa, promoting sustainable development.

Acknowledgement, The technical inputs of Mr Philips Amoo of Centre of Petroleum, Energy and Economics Department, University of Ibadan are acknowledged.
Disclosure statement: *Conflict of Interest:* The authors declare that there are no conflicts of interest.

Compliance with Ethical Standards: This article does not contain any studies involving human or animal subjects.

References

Abdalla, A. A., Abdallah, A. A., Odeleke, O. B. (2023). Energy Security in Nigeria: Challenges and Prospects. *Journal of Arid Zone Economy*, 1, Issue 1, 101-111.

Abubakar, I. R. (2014). Abuja city profile. *Cities*, *41*, 81–91. https://doi.org/10.1016/j.cities.2014.05.008

Alaoui S. M., A. Abouatallah A., Salghi R., Amahmid Z., Bettouche J., Zarrouk A., Hammouti B. (2013), Impact assessment of deficit irrigation on yield and fruit quality in peachorchard, *Der Pharmacia Chemica*, 5 (3), 236-243

Allen, R. G. , Pererira, L. S. , Raes, D. , & Smith, M. (1998). Crop Evapotranspiration - Guidelines for Computing Crop Water Requirements (CWR) - FAO Irrigation and Drainage Paper 56. *FAO - Food and Agriculture Organization of United Nations, Rome*.

Bathaei, A., & Štreimikienė, D. (2023). Renewable Energy and Sustainable Agriculture: Review of Indicators. In *Sustainability (Switzerland)* (Vol. 15, Issue 19). Multidisciplinary Digital Publishing Institute (MDPI). https://doi.org/10.3390/su151914307

Brouwer, C., & Hiebloem, M. (1986). Irrigation Water Management: Irrigation Water Needs, Training Manual 3. In *rrigation Water Management: Training Manual No.1 - Introduction to Irrigation* (Provisional Edition, Vol. 3). Food and Agriculture Orgnization of the United Nations. https://www.fao.org/4/s2022e/s2022e08.htm#TopOfPage

Byiringiro, J., Chaanaoui, M., & Halimi, M. (2024). Heat transfer enhancement of a parabolic trough solar collector using innovative receiver configurations combined with a hybrid nanofluid: CFD analysis. Renewable Energy, 233, 121169. https://doi.org/10.1016/j.renene.2024.121169

Byiringiro, J., Chaanaoui, M., & Hammouti, B. (2025). Thermal performance enhancement of a novel receiver for parabolic trough solar collector. *Interactions*, 246(1), 1-14. https://doi.org/10.1007/s10751-024-02230-3

Byiringiro, J., Chaanaoui, M., Hammouti, B. (2025). Enhancement of thermal performance in parabolic trough solar Collectors: Investigation of three novel receiver configurations using advanced heat transfer fluids. *Solar Energy Materials and Solar Cells*, 293, 113833. https://doi.org/10.1016/j.solmat.2025.113833

Dastane, N. G. (1978). *Effective Rainfall in Irrigated Agriculture* (Vol. 25). FAO - Food and Agriculture of the United Nations. https://www.fao.org/4/x5560e/x5560e00.htm#Contents

Emezirinwune, M. U., Adejumobi, I. A., Adebisi, O. I., & Akinboro, F. G. (2024). Synergizing hybrid renewable energy systems and sustainable agriculture for rural development in Nigeria. *E-Prime - Advances in Electrical Engineering, Electronics and Energy*, *7*, 100492. https://doi.org/10.1016/j.prime.2024.100492

Laita M., Sabbahi R., Elbouzidi A., Hammouti B., Messaoudi Z., Benkirane R., Aithaddou H. (2024) Effects of Sustained Deficit Irrigation on Vegetative Growth and Yield of Plum Trees Under the Semi-Arid Conditions: Experiments and Review with Bibliometric Analysis, *ASEAN Journal of Science and Engineering*, 4(2), 167-190

Majeed, Y., Khan, M. U., Waseem, M., Zahid, U., Mahmood, F., Majeed, F., Sultan, M., & Raza, A. (2023a). Renewable energy as an alternative source for energy management in agriculture. In *Energy Reports*, 10, 344–359. Elsevier Ltd. https://doi.org/10.1016/j.egyr.2023.06.032

Majeed, Y., Khan, M. U., Waseem, M., Zahid, U., Mahmood, F., Majeed, F., Sultan, M., & Raza, A. (2023b). Renewable energy as an alternative source for energy management in agriculture. *Energy Reports*, *10*, 344–359. https://doi.org/10.1016/j.egyr.2023.06.032

Martin, D. L., Gilley, J. R., Dickey, G. L., Salch, N. O., Hackbart, C. A., Koluvek, P. K., & Hardy, L. A. (1993). Irrigation Water Needs. In Soil Conservation Service (SCS) (Ed.), *Part 623, National Engineering Handbook*. United States Department of Agriculture.

Omeje, E. E., Enete, A. A., Mukaila, R., Onah, O. G., Ukwuaba, I. C., & Onyekwe, C. N. (2024). Operationalisation of low-carbon energy for sustainable agricultural production among smallholder women farmers in Nigeria. *Energy and Climate Change*, *5*, 100159. https://doi.org/10.1016/j.egycc.2024.100159

Tanko, L., & Muhsinat, B. S. Y. (2014). Arable Crops Farmer's Adapation to Climate Change in Abuja, Federal Capital Territory. *Journal of Agricultural and Crop Research*, *2*(8), 152–159.

Ukoba, K., Yoro, K. O., Eterigho-Ikelegbe, O., Ibegbulam, C., & Jen, T. C. (2024). Adaptation of solar energy in the Global South: Prospects, challenges and opportunities. In *Heliyon* (Vol. 10, Issue 7). Elsevier Ltd. https://doi.org/10.1016/j.heliyon.2024.e28009

Umar, I.S., Chidozie, E.E., Mohammed, U., Tauheed, L.Y. (2018). Assement of Women Participation in Home Gardening in Abuja, Federal Capital Territory (FCT), Nigeria. *Journal of Agriculture and Environment*, *14*(1), 39–47.

World Weather Online. (2024). *Abuja Annual Weather Averages*. Data provided by WorldWeatherOnline.com

Zotarelli, L., Dukes, M. D., Romero, C. C., Migliaccio, K. W., & Morgan, K. T. (2013). *Step by Step Calculation of the Penman-Monteith Evapotranspiration (FAO-56 Method) 1*. http://fawn.

(2025) ; http://www.jmaterenvironsci.com